NASA Technical Paper 2291

March 1984

An Assessment of the Capability To Calculate Tilting Prop-Rotor Aircraft Performance, Loads, and Stability

Wayne Johnson

NASA

NASA
Technical
Paper
2291

1984

An Assessment of the Capability To Calculate Tilting Prop-Rotor Aircraft Performance, Loads, and Stability

Wayne Johnson

Ames Research Center
Moffett Field, California

NASA
National Aeronautics
and Space Administration

**Scientific and Technical
Information Branch**

TABLE OF CONTENTS

NOMENCLATURE

a	mean line designation parameter for NACA 6-series airfoils
A	rotor disk area, πR^2
$c_{d_{\min}}$	airfoil minimum drag coefficient
$c_{\ell_{\max}}$	airfoil maximum lift coefficient
c_{ℓ_α}	airfoil lift curve slope
C_{f_c}	pitch link load coefficient, $NF_c/\rho A(\Omega R)^2$
C_{m_x}	blade beamwise bending moment coefficient, $NM_x/\rho A(\Omega R)^2 R$
C_{m_z}	blade chordwise bending moment coefficient, $NM_z/\rho A(\Omega R)^2 R$
C_P	rotor power coefficient, $P/\rho A(\Omega R)^3$
C_T	rotor thrust coefficient, $T/\rho A(\Omega R)^2$
D	airframe drag
f	airframe equivalent drag area (drag divided by dynamic pressure)
F_c	blade pitch link load
L	airframe lift
M	Mach number (velocity divided by speed of sound)
M	rotor figure of merit, $C_T^{3/2}/\sqrt{2}\,C_P$
M_{tip}	rotor tip Mach number (tip speed ΩR divided by speed of sound)
M_x	blade beamwise bending moment
M_z	blade chordwise bending moment
N	number of blades per rotor
P	rotor power
q	dynamic pressure, $\rho V^2/2$
r	radial distance along rotor blade
R	rotor radius
T	rotor thrust
V	aircraft or wind tunnel speed
α_P	pylon tilt angle; 0 for airplane mode, 90° for helicopter mode
ζ	modal damping ratio
η	propulsive efficiency, TV/P
κ_f	empirical factor for induced velocity calculation in helicopter forward flight
κ_h	empirical factor for induced velocity calculation in hover
ρ	air density
σ	rotor solidity (ratio total blade area to rotor disk area)
ω	modal frequency
Ω	rotor rotational speed

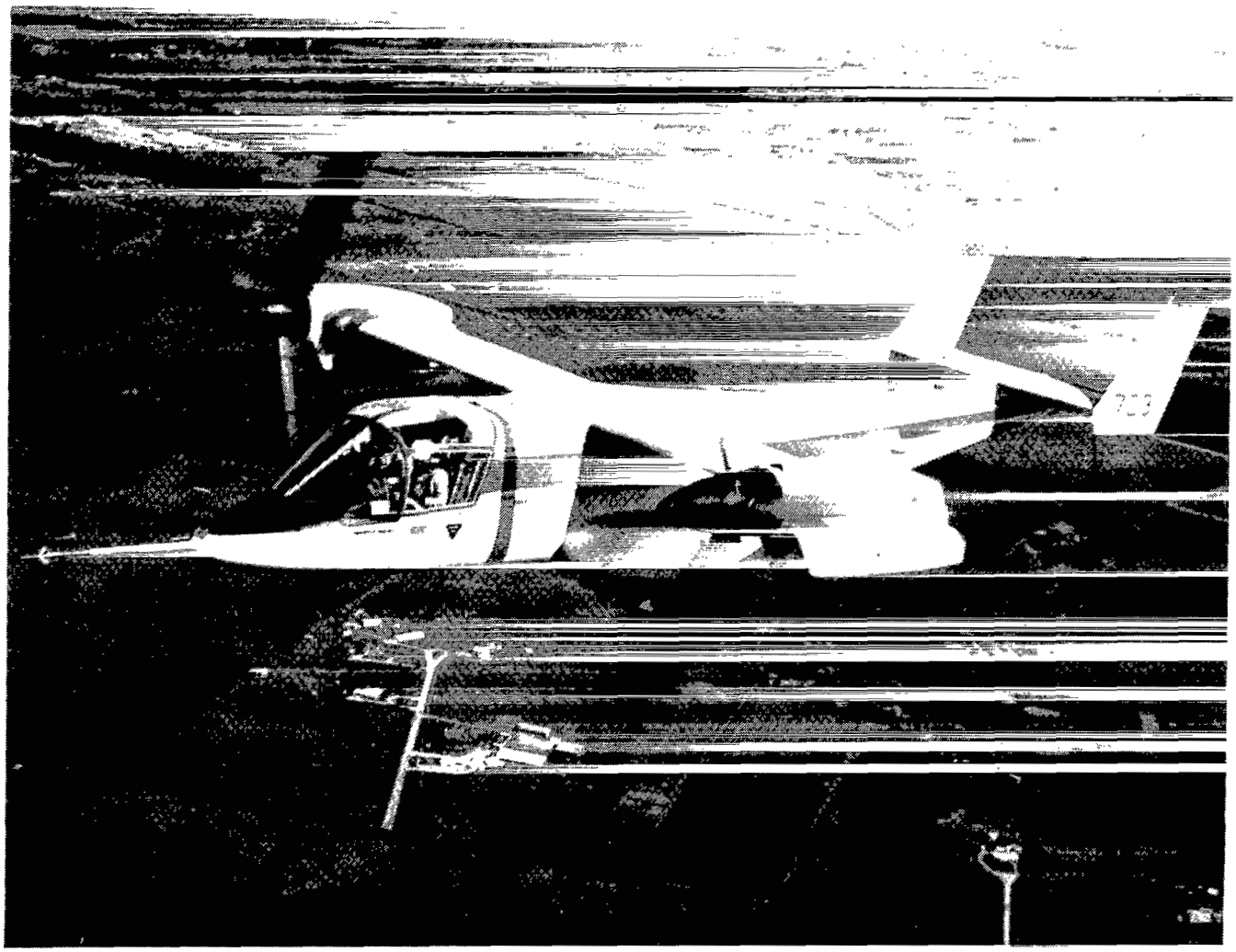

Figure 1.– XV-15 Tilt Rotor Research Aircraft in airplane configuration.

SUMMARY

Calculated performance, loads, and stability of the XV-15 Tilt Rotor Research Aircraft are compared with wind-tunnel and flight measurements, to define the level of the current analytical capability for tilting prop-rotor aircraft, and to define the requirements for additional experimental data and further analysis development. The correlation between calculated and measured behavior is generally good, although there are some significant discrepancies. Based on this correlation, the analysis used is assessed overall as being adequate for the design, evaluation, and testing of tilting prop-rotor aircraft. A general assessment of the state of the art of tilt rotor predictive capability is given. Specific areas are identified where improvements in the capability to calculate performance, loads, and stability are desirable. Requirements for more accurate and detailed data which support the development of improved analytical models are identified as well.

INTRODUCTION

The XV-15 Tilt Rotor Research Aircraft was developed to demonstrate the solution of the key technical problems of this aircraft configuration. With the successful conclusion of the proof-of-concept flight tests of the XV-15, attention is now focused on the next generation of tilt rotor designs. To enable development of future tilting prop-rotor aircraft, there is a requirement for accurate prediction techniques which can be verified by the currently available XV-15 test data. The purpose of this paper is to assess the current capability to calculate performance, loads, and stability of tilting prop-rotor aircraft.

These calculations were performed using a comprehensive analysis (refs. 1 and 2) designed to handle tilt rotor aircraft as well as helicopter configurations. This analysis provides performance, blade loads, and aeroelastic stability from a single, consistent analytical formulation. The calculations are compared with wind-tunnel and flight measurements for the XV-15, to verify the use of the analysis in the design, evaluation, and testing of tilt rotor aircraft. The objective of the paper is to define the level of the current analytical capability for tilting prop-rotor aircraft, and to identify where additional experimental data and further analysis development are desirable.

AIRCRAFT

The XV-15 Tilt Rotor Research Aircraft in flight is shown in figures 1 and 2. The principal parameters describing the aircraft and the rotor system are given in table 1. A complete description of the geometric, structural, inertial, and aerodynamic characteristics are given in references 3-6. The XV-15 has been flight tested by NASA and Bell Helicopter since 1978, and data on the performance, blade loads, and aeroelastic stability are now available. The rotor alone was tested full scale in the Ames Research Center 40- by 80-Foot Wind Tunnel during 1970. The rotor was tested on a powered stand for performance and loads data (fig. 3) with the overhead doors open for hover tests, and was tested while windmilling, on a cantilever wing, for stability data (fig. 4). The flight-test data presented in this report were obtained from the Tilt Rotor Aircraft Office at NASA-Ames Research Center, and from Bell Helicopter. The wind-tunnel data were obtained from reference 7.

ANALYTICAL MODEL

The analysis used to perform the calculations presented in this report is described in detail in references 1 and 2. The minimum required level of modeling complexity is different for the performance, loads, and stability problems. The requirements for a sufficient model are established by varying the relevant parameters, such as the number of degrees of freedom. Here it is also necessary to consider the differences between the aircraft and the rotor alone, which are reflected primarily in the trim procedure and in the degrees of freedom for the stability calculation.

Degrees of Freedom and Analysis Parameters

The degrees of freedom used in the calculations are shown in table 2. The performance and loads results require a

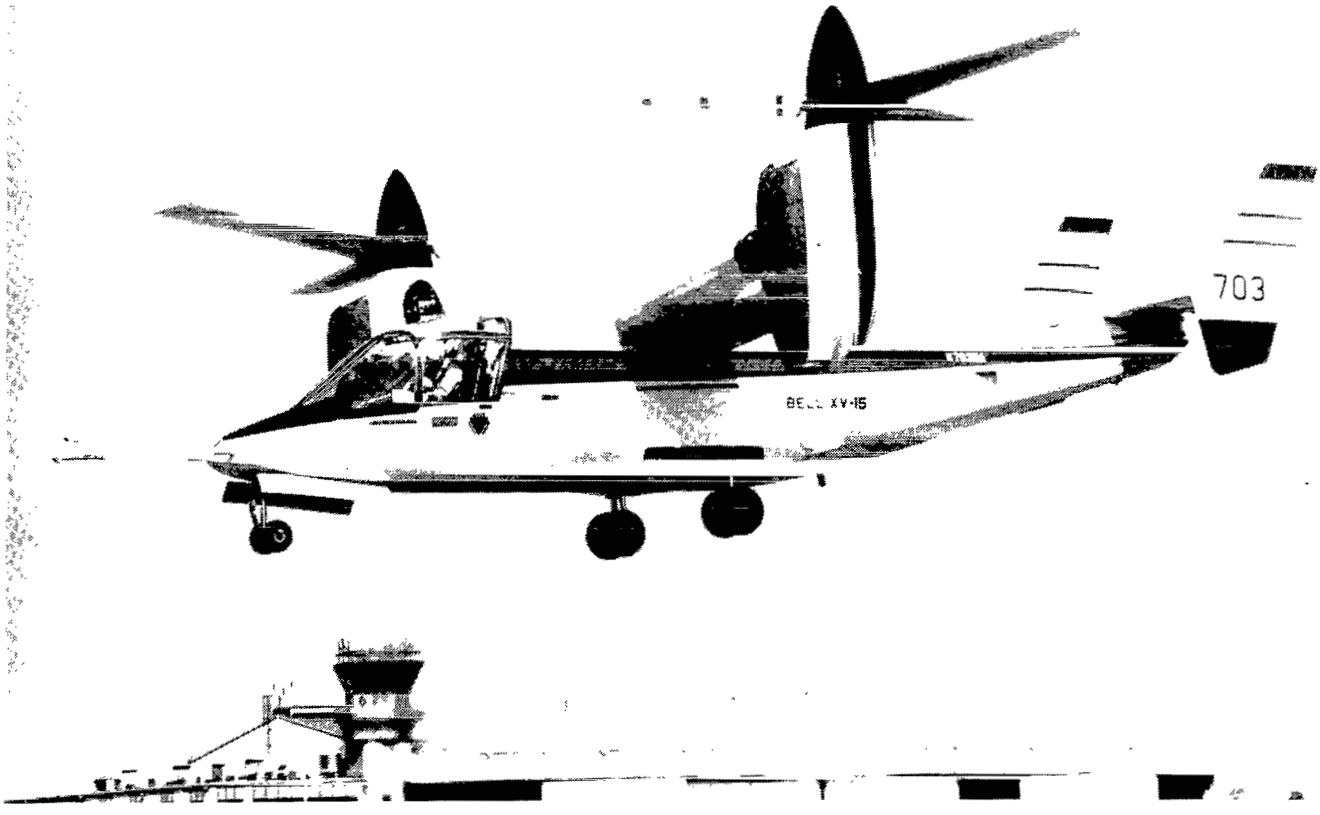

Figure 2.– XV-15 Tilt Rotor Research Aircraft in helicopter configuration.

solution for the periodic rotor motion, whereas the stability solution involves the perturbed motion of the rotor and the airframe. Ten harmonics were used in the periodic motion solution when calculating blade loads; one harmonic was generally sufficient for the performance calculations. An azimuthal increment of 15° was used in the periodic motion solution. Fifteen radial stations, concentrated at the blade tip, were used for the aerodynamic analysis of the rotor.

TABLE 1.– XV-15 TILT ROTOR RESEARCH AIRCRAFT PARAMETERS

Configuration	Side-by-side, tilt nacelle
Number of rotors	2
Wing span	9.80 m
Design gross weight	5900 kg
Engines	Two modified Lycoming T53-L13B
Normal rated power	930 W each
Rotor type	Gimballed, stiff inplane
Number of blades	3
Radius	3.81 m
Solidity	0.089
Lock number	3.67
Pitch/flap coupling	-15°
Precone	2.5°
Tip airfoil	NACA 64-208 (a = 0.3)
Root airfoil	NACA 64-935 (a = 0.3)

There was little effect shown in the calculations of the blade loads when two to six bending modes or zero to two elastic torsion modes were used. Hence the minimum model consisted of two bending modes plus the rigid pitch motion. The rigid-pitch degree of freedom had a considerable influence, especially on the calculated oscillatory pitch-link loads.

A detailed discussion of the analytical model required for stability calculations is given in reference 4. The conclusion of that work was that the minimum model for the rotor consists of two bending modes and the rigid-pitch motion per blade, as well as the gimbal and rotor-speed degrees of freedom.

When two to six bending modes were used, little effect was shown in the calculations of the rotor performance. Blade bending is not expected to be a factor in the consideration of the key performance conditions for the tilt-rotor configuration, namely hover and high-speed cruise, which are both axisymmetric operating conditions for the rotor. A

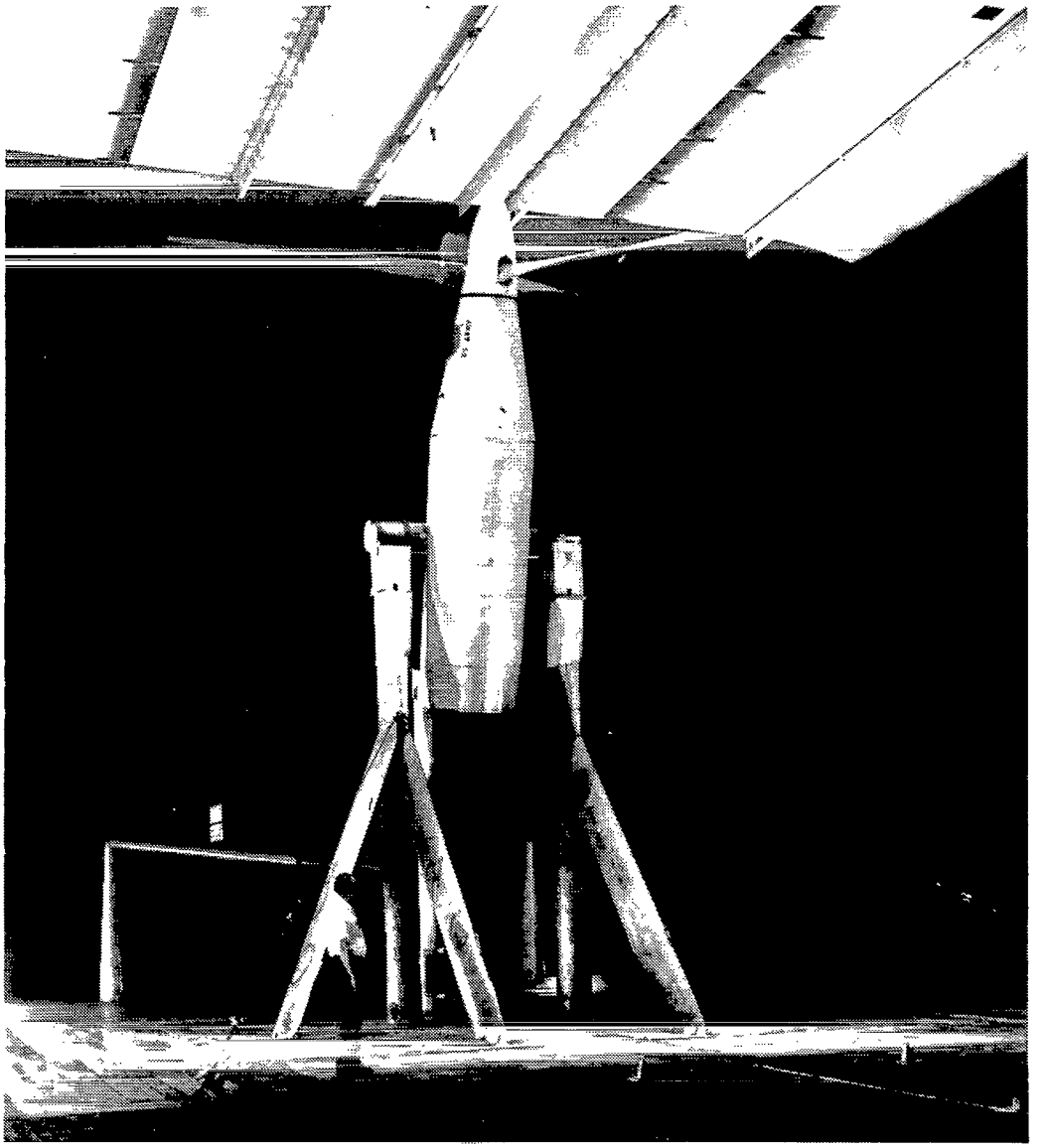

Figure 3.– XV-15 rotor on powered test stand in the Ames 40- by 80-Foot Wind Tunnel (overhead doors were open for hover tests).

significant steady rigid-pitch deflection of the blade was calculated (typically 1-2°, caused by control system flexibility), but such motion only produces a change in the collective control for a given thrust. Little effect was seen in the calculated performance in hover when using zero to two elastic torsion modes. In airplane mode flight however, the calculation showed about 1.5% better performance when the first elastic torsion mode was used. Little effect was seen when using higher elastic torsion modes, and no coupling of this phenomenon with any bending modes was evident. A typical result was an elastic torsion deflection of -1.2° at the blade tip, for $V/\Omega R = 0.7$, and for $C_T/\sigma = 0.025$. This twist change produces a favorable redistribution of the blade loading. Hence, the influence of the steady-blade torsion deflection on the calculated performance is not negligible. However, it will be seen that the effect for the XV-15 does not significantly improve the correlation between the calculations and the experimental data. By using a reduced blade-torsion stiffness and an aft placement of the chordwise location of the aerodynamic center, these analytical results imply that it is possible to design a rotor for a significant performance improvement because of the static torsion deflection. At least 5% better propulsive efficiency in airplane configuration can be achieved, with no penalty on hover figure of merit. However, such a change in the rotor design would reduce the flutter speed.

Figure 4.– XV-15 rotor on dynamics test stand in the Ames 40- by 80-Foot Wind Tunnel.

Aerodynamics

Static, two-dimensional airfoil characteristics were used in the analysis, with corrections for yawed flow effects and a tip loss factor (ref. 2). The airfoil data is given in reference 7. The airfoil lift-curve slope is a key parameter for the stability calculations. The maximum lift coefficient and the minimum drag coefficient are particularly important for the loads and performance. The variations of these parameters with Mach number are shown in figure 5.

For the stability calculations, a quasistatic perturbation of the uniform rotor inflow was used as a model of the rotor wake influence on the unsteady aerodynamics (refs. 1 and 2). However, such inflow perturbations have little influence on the stability for a gimballed rotor.

The rotor wake-induced velocity used in the calculations was constant over the rotor disk for hover and cruise (axial flow conditions), and varied linearly over the rotor disk for helicopter forward flight. The mean induced velocity was

TABLE 2.– DEGREES OF FREEDOM USED IN CALCULATIONS

	Periodic motion		Perturbation motion	
	Performance	Loads	Cantilever stability	Airplane stability
Rotor				
Gimbal pitch and roll	Yes	Yes	Yes	Yes
Rotational speed	None	None	Yes	Yes
Each blade				
Coupled flap/lag bending	2 modes	3 modes	2 modes	2 modes
Rigid pitch motion	None	Yes	Yes	Yes
Elastic torsion	None	1 mode	None	None
Airframe				
Rigid body	None	None	None	3 symmetric or 3 antisymmetric motions
Elastic	None	None	3 modes	4 symmetric or 4 antisymmetric modes
Total number	3	6	15	19

obtained from momentum theory, with the ideal value multiplied by the factor $\kappa_h = 1.17$ in hover, and $\kappa_f = 2.0$ in helicopter forward flight. These empirical factors account for nonideal induced-power losses (see ref. 2), which may be expected to be larger for this rotor than for conventional helicopter rotors, particularly because of its high twist.

No significant improvement in the general correlation of the performance and loads calculations was obtained using the nonuniform inflow or dynamic stall models described in references 1 and 2. Nonuniform inflow and dynamic stall do influence the details of the calculated behavior, and good models for these phenomena would be expected to improve the prediction accuracy. The currently available analytical models offer little improvement for tilt rotor calculations relative to using uniform inflow and static stall. For example, calculations of hover performance produced inconsistent results when an existing prescribed wake geometry model was used. The power calculations at low and high thrust were good, but at moderate thrusts the calculated induced power was actually less than the ideal loss. Such behavior is not surprising since the wake geometry model was developed for helicopter rotors, not for the highly twisted blades of a tilt rotor. Other state-of-the-art analyses produce similar results. One prescribed wake geometry analysis currently in use by industry provides calculated performance that shows correct trends but is too optimistic. The analysis was developed for helicopters, and it shows induced power levels typical of helicopters rather than tilt rotors. Another analysis which is being used by industry gives good performance predictions up to moderate thrusts, but predicts stall of the rotor too soon, so the predicted maximum lift of the rotor is far less than observed in tests. Hence, a uniform inflow model represents the current state of the art for tilting prop-rotor aircraft.

Airframe Model

The XV-15 airframe aerodynamics are described in the analysis by a drag of $D/q = 0.84 + 0.0040(L/q)^2$ m^2, and a hover download of 11%. These values are based on correlation with the flight-test data, as discussed below. While direct measurements of the drag and download are not available, there are independent estimates from model tests that support these values to at least ±20%. The mode shapes and generalized mass of the airframe and cantilever wing used in the stability analysis were obtained from NASTRAN (finite element) calculations provided by Bell Helicopter. The frequency and structural damping of the modes were matched to the measured values, although results will also be shown using the NASTRAN frequencies. The calculations using the NASTRAN frequencies and a nominal structural damping level will be called pretest results. The calculations using measured frequencies and structural damping levels will be called post-test results. A blade rigid-pitch natural frequency of 36 Hz was used, based on reference 7. Higher values of the control system stiffness would decrease the calculated control loads and raise the stability boundary.

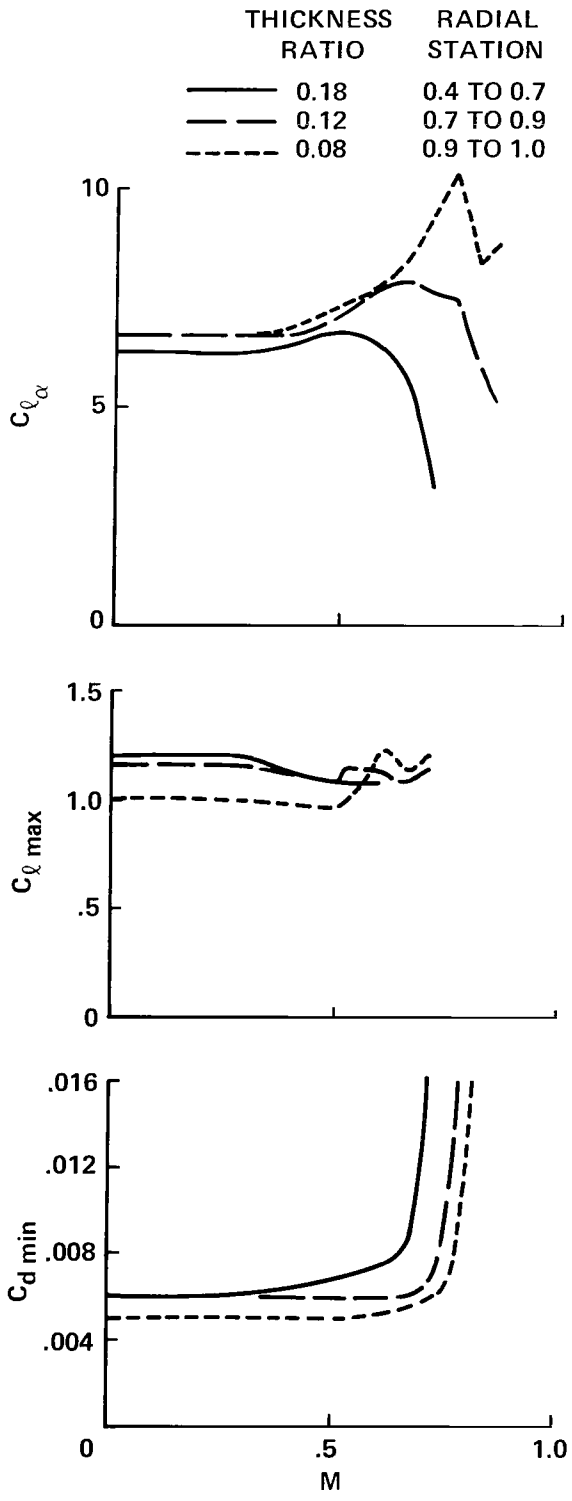

Figure 5.– Variation with Mach number of lift curve slope, maximum lift coefficient, and minimum drag coefficient from XV-15 rotor airfoil tables.

Trim Analysis

The aircraft was trimmed in the analysis to symmetric, level flight at a given speed, by adjusting the pilot's controls and aircraft attitude. For the performance and loads calculations in the wind tunnel, the rotor was trimmed to a specified thrust and to zero longitudinal flapping angle by adjusting the collective pitch and longitudinal cyclic-pitch controls. At pylon angles of 0° and 5°, the cyclic control was zero and only the rotor thrust was trimmed. For the calculations of stability in the wind tunnel (for which the rotor was windmilling) the torque was trimmed to zero by adjusting the collective pitch.

PERFORMANCE RESULTS

The performance of the XV-15 Tilt Rotor Research Aircraft in cruise flight is shown in figures 6 to 9. The rotor is operating in axial flow, functioning as a propeller. Figure 6 shows the rotor propulsive efficiency as a function of thrust, with good correlation between the calculations and the full scale wind-tunnel test results. The measured data show no systematic influence of either speed or tip Mach number (although the maximum resultant tip Mach number achieved was only 0.69). The theory confirms the small influence of $V/\Omega R$. Figure 7 shows the influence of the static-elastic torsion deflection of the rotor blade. The effect is small, but not

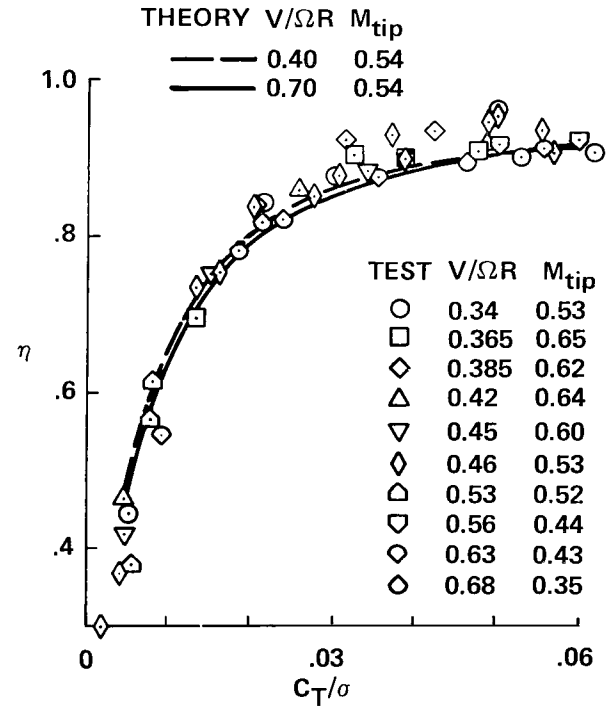

Figure 6.– Rotor propulsive efficiency as a function of thrust; comparison of wind-tunnel test and calculated results.

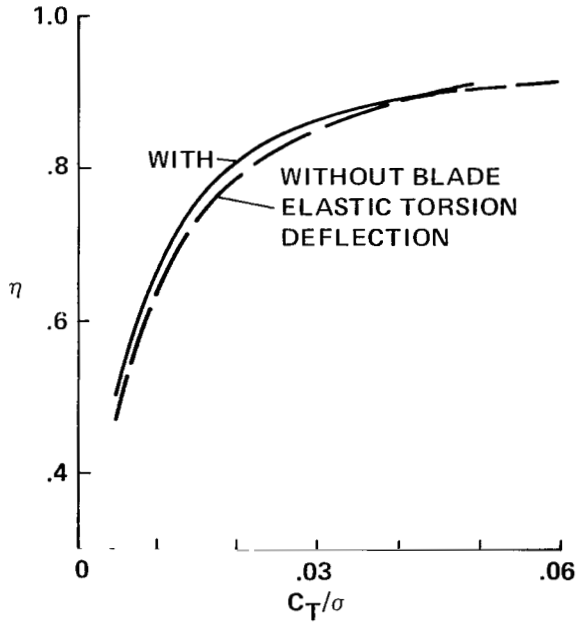

Figure 7.– Influence of static torsion deflection on calculated rotor propulsive efficiency ($V/\Omega R$ = 0.70 and M_{tip} = 0.54).

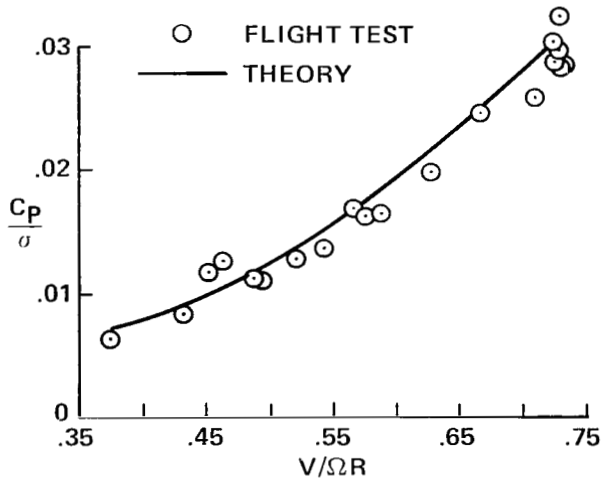

Figure 8.– Rotor power as a function of speed, for M_{tip} = 0.60; comparison of flight-test and calculated results.

negligible. The influence of the torsion deflection is in the direction to slightly improve the correlation shown in figure 6 (which does not include the torsion effect).

Figure 8 presents the rotor power as a function of speed, and figure 9 shows the same data in terms of propulsive efficiency. Good correlation between flight-test results and calculations is shown, as well as between flight and wind-tunnel tests results. This correlation was achieved by using an equivalent drag area of f = 0.84 m^2 for the airframe. While further analysis of the flight-test data may make it possible to improve the correlation, little more can be concluded about the capability to predict tilt rotor characteristics without direct wind-tunnel measurements of the airframe drag.

The performance of the XV-15 in hover is shown in figures 10 and 11. Figure 10 gives the hover figure of merit as a function of thrust, whereas figure 11 gives the same results in terms of power coefficient. By using an empirical factor of κ_h = 1.15 to 1.17 in the induced velocity calculation, good correlation is achieved between the wind-tunnel test results and the theory. However, the data show considerable scatter, particularly in terms of the figure of merit. Hover data from out-of-ground-effect flight tests are also shown in figures 10 and 11. Good correlation with the wind-tunnel and calculated results is shown, based on a download of 11%. Good agreement between the flight-test data and theory is obtained if a value for the hover-induced velocity factor of κ_h = 1.15, 1.17, or 1.19 is used, together with a download of 12%, 11%, or 10%, respectively. Comparison of the calculations with the

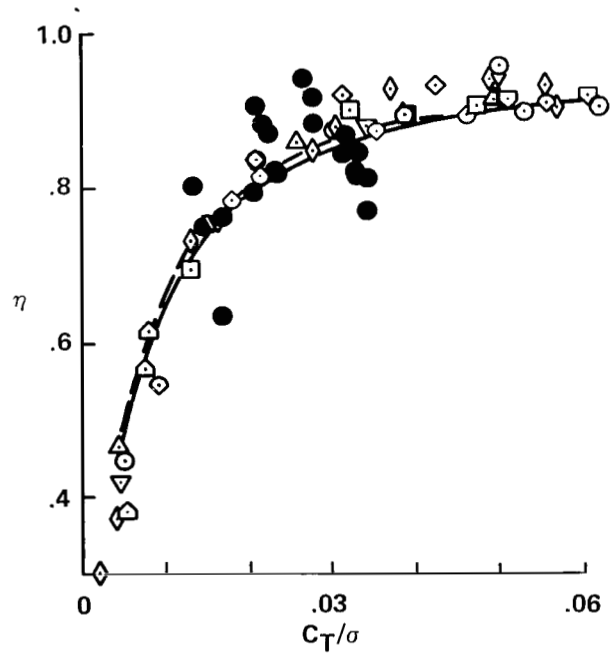

Figure 9.– Comparison of rotor propulsive efficiency from flight test (solid symbols), wind-tunnel test (open symbols), and theory (lines; see fig. 6 for key).

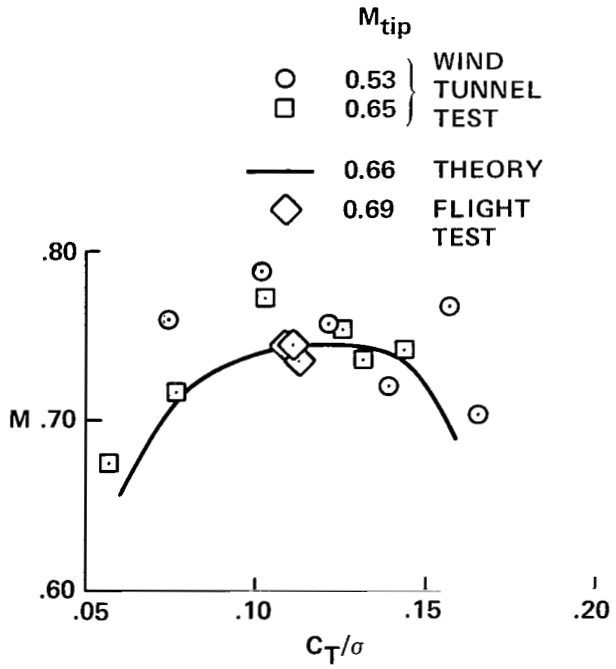

Figure 10.– Rotor hover figure of merit as a function of thrust; comparison of flight test, wind-tunnel test, and theory.

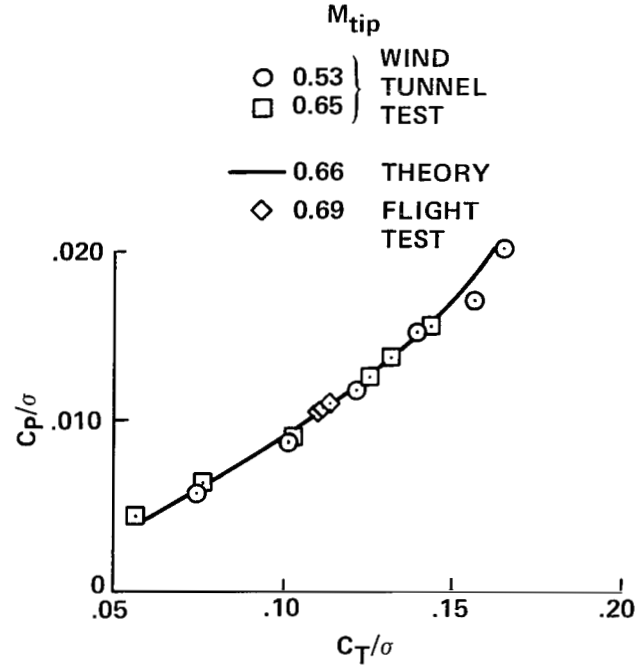

Figure 11.– Rotor hover power as a function of thrust; comparison of flight test, wind-tunnel test, and theory.

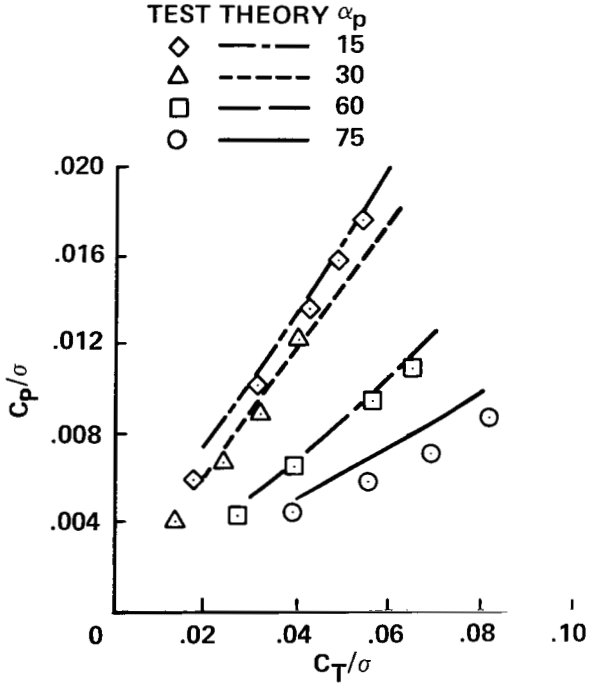

Figure 12.– Rotor power as a function of thrust, for $V/\Omega R = 0.32$ and $M_{tip} = 0.65$; comparison of wind-tunnel test and calculated results.

wind-tunnel data indicates that the appropriate value of κ_h is at the low end of this range, and hence it is concluded that the download is 11% to 12%. It should be noted that wing configurations to reduce the download are currently being investigated.

The appropriate value for κ_h is deduced by comparing the theoretical calculations and the wind-tunnel test data. The result depends on the airfoil data being used, however, since the sum of the profile power (depending on the airfoil drag) and the induced power (depending on κ_h) must match the total measured power. Hence, if the drag level in the airfoil table were higher, a smaller value of κ_h would be required to achieve the same correlation shown in figures 10 and 11. The appropriate value for the wing download is deduced by comparing the flight- and wind-tunnel test data, and hence, is independent of the split between profile and induced power in the predicted hover performance.

Wind-tunnel results for the rotor power at pylon tilt angles from 15° to 75° are presented in figures 12 and 13. The power is well predicted for $\alpha_P = 0°$ to 60° (airplane and tilt rotor configurations), but is overpredicted at $\alpha_P = 75°$ (helicopter forward flight). An induced power loss less than that predicted is not probable (as is confirmed by nonuniform inflow calculations), so the profile power is being overpredicted. This can be attributed to deficiencies in the stall model since the inboard portion of this highly twisted blade is stalled at $\alpha_P = 75°$ even for moderate thrust.

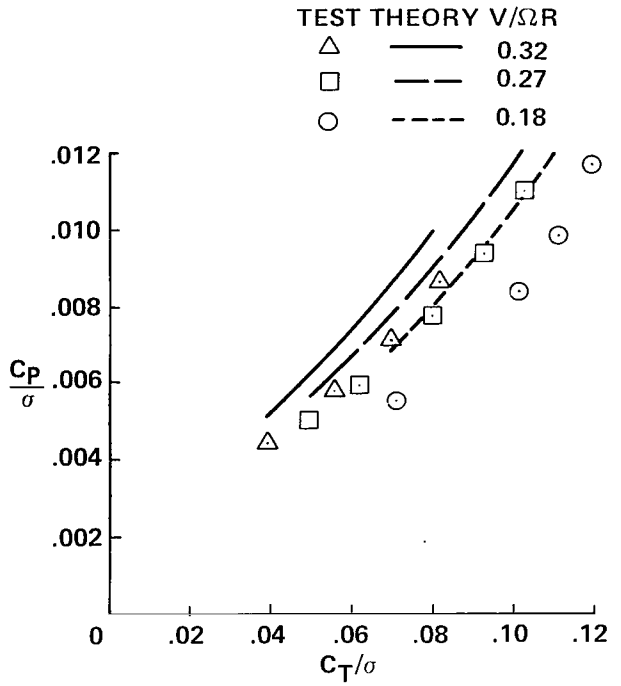

Figure 13.– Rotor power as a function of thrust, for $\alpha_P = 75°$ and $M_{tip} = 0.65$; comparison of wind-tunnel test and calculated results.

ROTOR LOADS RESULTS

The critical rotor loads for the XV-15 are identified (ref. 7) as follows: the oscillatory beamwise bending moment at $0.35R$ radial station (C_{m_x}/σ); the oscillatory spindle chord bending moment, at approximately $0.05R$ (C_{m_z}/σ); and the oscillatory pitch-link force (C_{f_c}/σ). The oscillatory load is defined as one-half the difference between the maximum and minimum load values occurring in a rotor revolution. The beamwise bending moment is measured relative to the blade principal axes (rotated by the local pitch angle relative to shaft axes). The spindle chord moment is measured just inboard of the blade pitch bearing and outboard of the spindle/yoke junction, relative to the rotor shaft axes.

The calculated XV-15 rotor loads are compared with full scale wind-tunnel measurements in figures 14 to 23. The oscillatory bending moments as a function of blade radial station are shown in figures 14 and 15. The moments inboard of $r/R = 0.1$ are relative to the shaft axes, while the moments outboard of $r/R = 0.1$ are relative to the local blade principal axes. The correlation is generally good, although the predicted beamwise bending moment is somewhat low at $r/R = 0.16$.

The measured and calculated oscillatory loads as a function of thrust are compared in figures 16 to 18 for the beamwise bending moment at $0.35R$; in figures 19 and 20 for the spindle chord bending moment; and in figures 21 to 23 for the pitch-link load. The loads are presented for three speeds at a nacelle angle of 75°; for four nacelle angles at $V/\Omega R = 0.32$; and for two nacelle angles at $V/\Omega R = 0.51$. (Spindle chord load data are not available for the last case.) The tip Mach number was 0.65 for nacelle angles from 15° to 75°, and 0.53 for nacelles angles of 0° and 5°.

The oscillatory beamwise bending moments are predicted well in figure 16, although the loads increase somewhat faster than predicted at the highest thrust. The predicted loads at $V/\Omega R = 0.32$ (fig. 17) are high for $\alpha_P = 60°$ and are low for

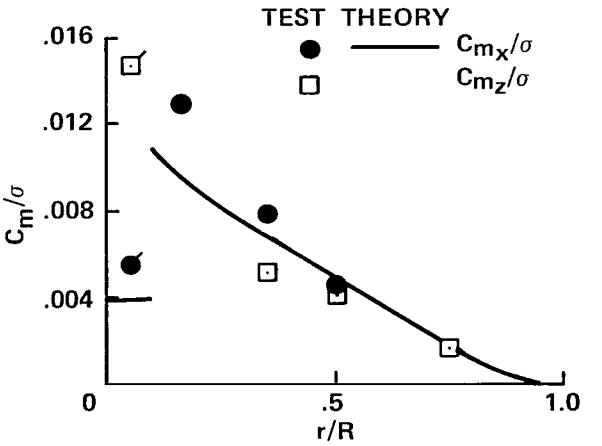

Figure 14.– Oscillatory beamwise bending moment as a function of radial station for $\alpha_P = 75°$, $M_{tip} = 0.65$, $V/\Omega R = 0.27$, and $C_T/\sigma = 0.102$ (flagged symbols are measurements on spindle); comparison of wind-tunnel test and calculated results.

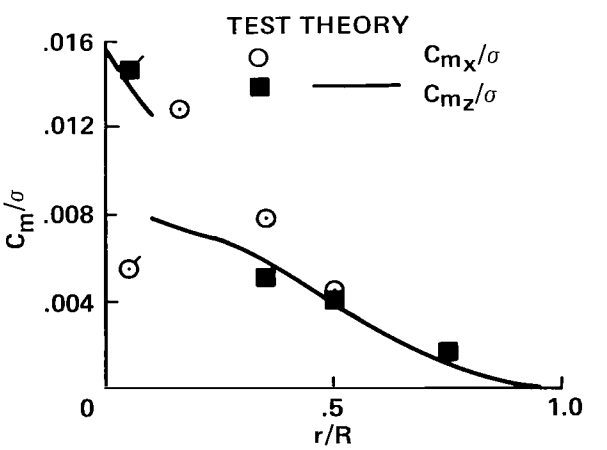

Figure 15.– Oscillatory chordwise bending moment as a function of radial station for $\alpha_P = 75°$, $M_{tip} = 0.65$, $V/\Omega R = 0.27$, and $C_T/\sigma = 0.102$ (flagged symbols are measurements on spindle); comparison of wind-tunnel test and calculated results.

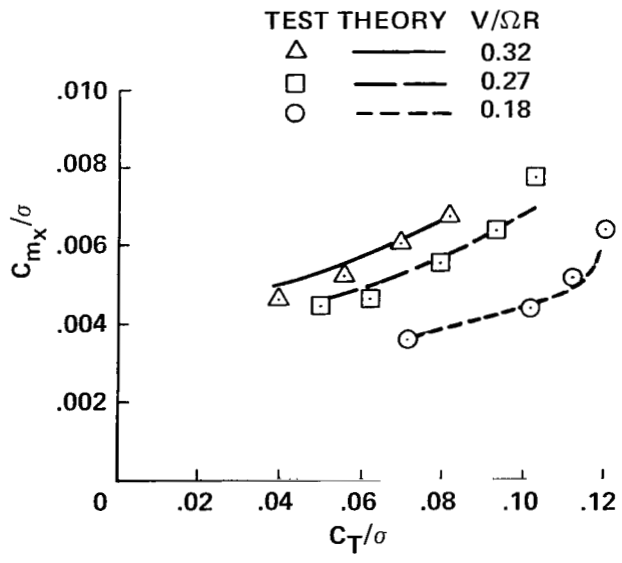

Figure 16.– Oscillatory beamwise bending moment at 0.35R as a function of thrust for α_P = 75° and M_{tip} = 0.65; comparison of wind-tunnel test and calculated results.

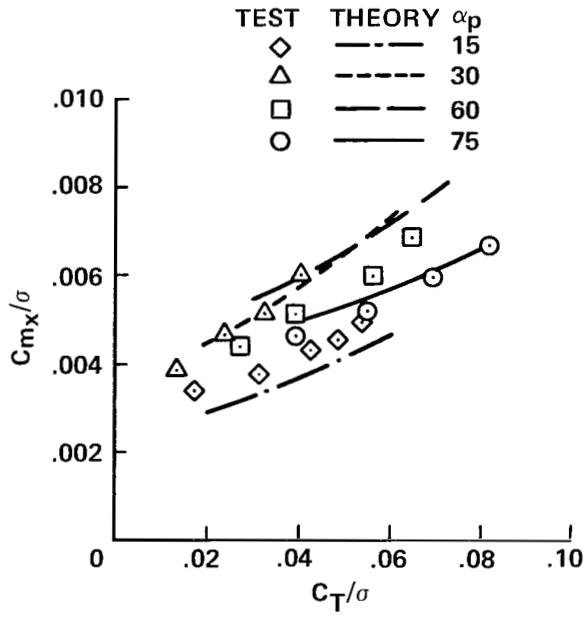

Figure 17.– Oscillatory beamwise bending moment at 0.35R as a function of thrust for M_{tip} = 0.65 and $V/\Omega R$ = 0.32; comparison of wind-tunnel test and calculated results.

α_P = 15°; the slope with thrust is predicted well for all four nacelle angles. The predicted loads are low for α_P = 0° and 5° (fig. 18) but the magnitude of the loads is small in the airplane configuration.

The oscillatory spindle chord bending moments are predicted well in figure 19, except for the results at $V/\Omega R$ = 0.32 and high thrust. That the measured loads at $V/\Omega R$ = 0.32 are as low as the loads at $V/\Omega R$ = 0.27 is unexpected, however. The predicted loads are low for α_P = 15° (fig. 20).

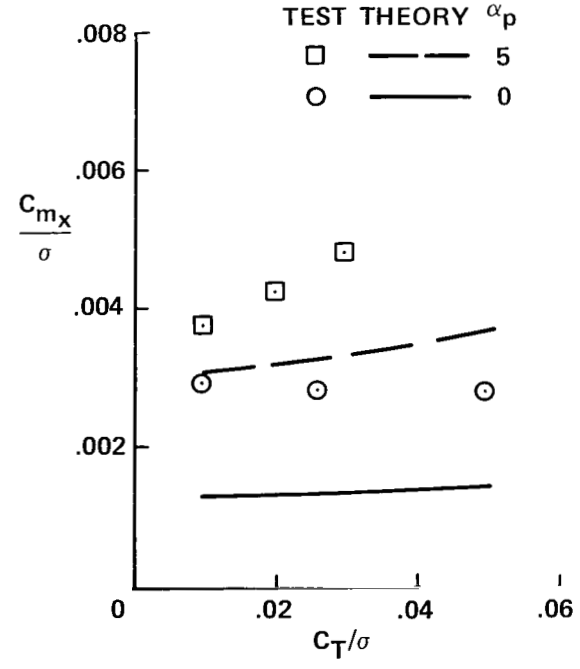

Figure 18.– Oscillatory beamwise bending moment at 0.35R as a function of thrust for M_{tip} = 0.53 and $V/\Omega R$ = 0.51; comparison of wind-tunnel test and calculated results.

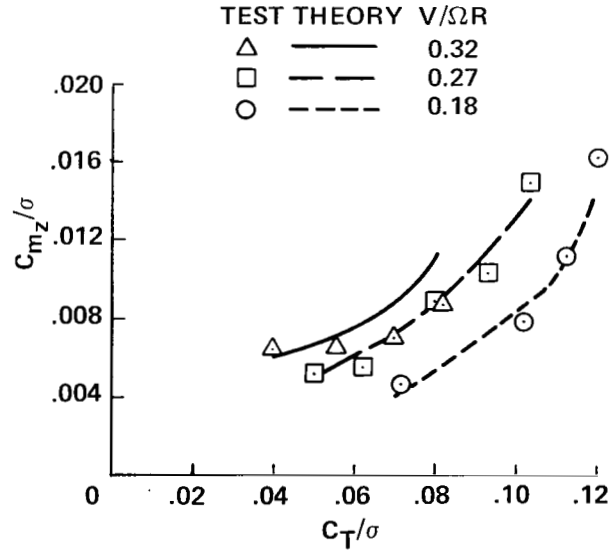

Figure 19.– Oscillatory spindle chord bending moment as a function of thrust for α_P = 75° and M_{tip} = 0.65; comparison of wind-tunnel test and calculated results.

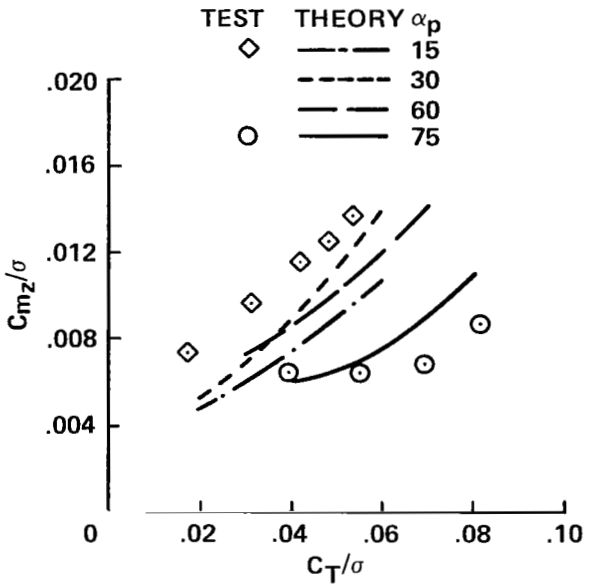

Figure 20.– Oscillatory spindle chord bending moment as a function of thrust for M_{tip} = 0.65 and $V/\Omega R$ = 0.32; comparison of wind-tunnel test and calculated results.

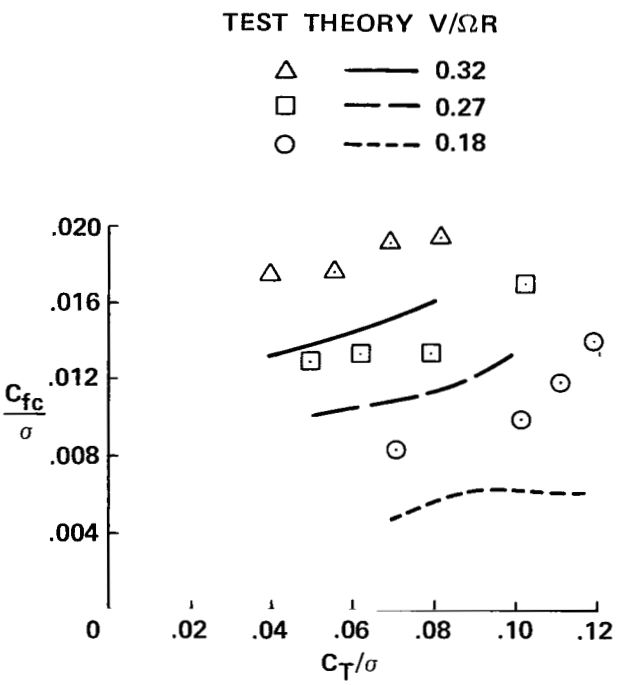

Figure 21.– Oxcillatory pitch-link load as a function of thrust for α_P = 75° and M_{tip} = 0.65; comparison of wind-tunnel test and calculated results.

The oscillatory pitch-link loads are underpredicted by about 250 to 300 N for all cases (figs. 21 to 23), including the nominally axial flow condition to α_P = 0 (fig. 23). The source of the oscillatory pitch-link loads at zero nacelle incidence is not known, but it appears to be extant for all operating conditions. It is also noted that for $V/\Omega R$ = 0.18 (fig. 21), the increase in pitch-link load at high thrust (presumably because of stall) is not predicted.

The calculated XV-15 rotor loads are compared with flight-test results in figures 24 to 26. The oscillatory bending loads are shown as a function of speed for five pylon angles, and the oscillatory pitch-link loads are shown for three pylon angles. The aircraft was operating at a gross weight of 5900 kg; a center-of-gravity fuselage station of 7.623 m; altitudes from 750 to 1,500 m; and with a rotor tip Mach number of 0.65.

The oscillatory beamwise bending moment is predicted well (fig. 24). Both the trends and magnitude of the calculations are correct, although the predictions are somewhat high for α_P = 75° and 60°. The oscillatory chordwise bending moment in flight is generally not predicted well (fig. 25). While the results of the theory are good for α_P = 75°, they are somewhat high for α_P = 60°, and for α_P = 30° they are low and the slope is too small. The predictions for α_P = 90° are low, and in particular do not exhibit the growth at speeds above $V/\Omega R$ = 0.2 that is evident in the data. The predictions for α_P = 0 are very low; the data for zero nacelle incidence is

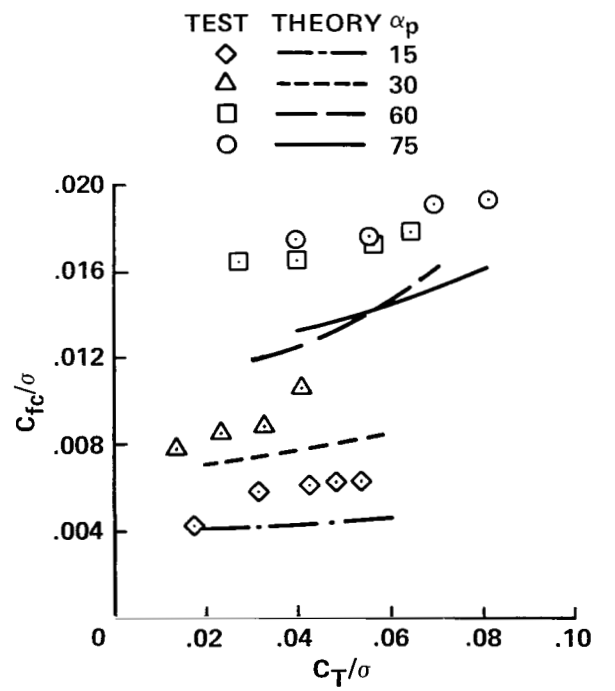

Figure 22.– Oscillatory pitch-link load as a function of thrust for M_{tip} = 0.65 and $V/\Omega R$ = 0.32; comparison of wind-tunnel test and calculated results.

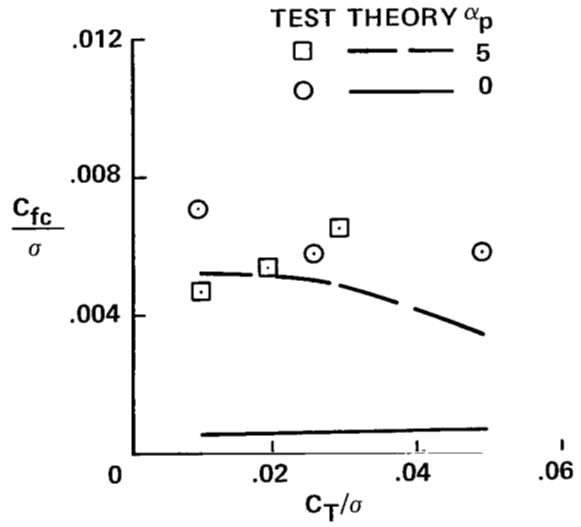

Figure 23.– Oscillatory Pitch-link load as a function of thrust for M_{tip} = 0.53 and $V/\Omega R$ = 0.51; comparison of wind-tunnel test and calculated results.

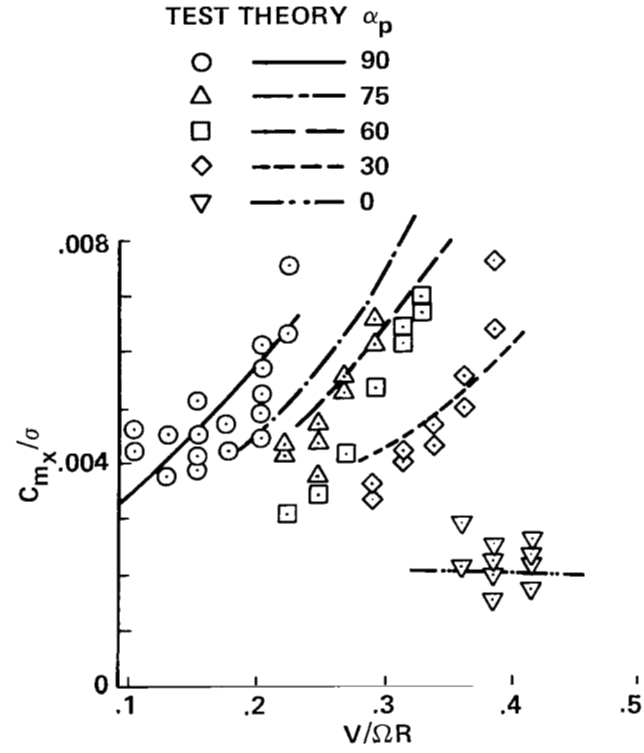

Figure 24.– Oscillatory beamwise bending moment at 0.35R as a function of speed for M_{tip} = 0.65; comparison of flight test and calculated results.

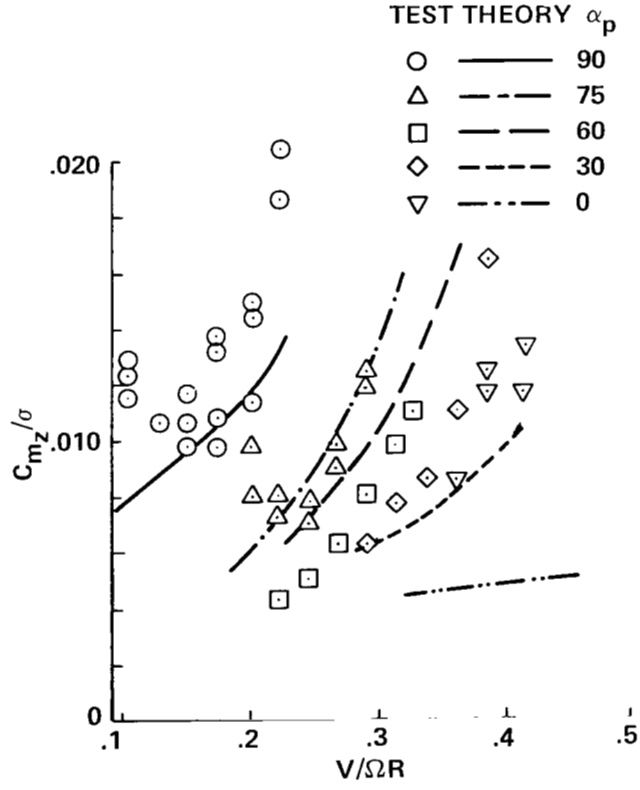

Figure 25.– Oscillatory spindle chord bending moment as a function of speed for M_{tip} = 0.65; comparison of flight test and calculated results.

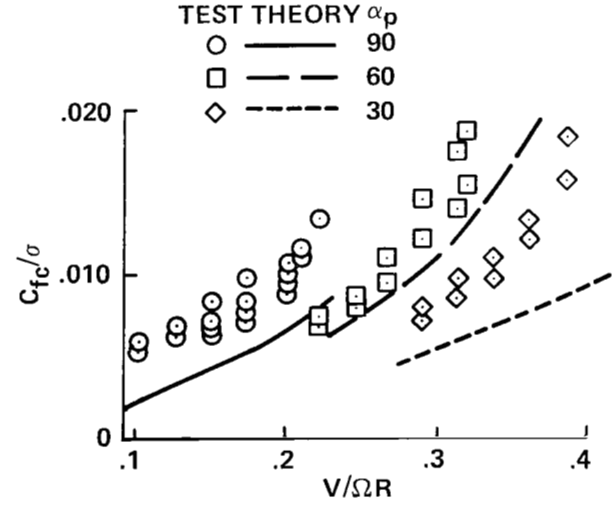

Figure 26.– Oscillatory pitch-link load as a function of speed for M_{tip} = 0.65; comparison of flight test and calculated results.

about the same as for $\alpha_P = 30°$. The discrepancies in helicopter forward flight ($\alpha_P = 90°$) are probably caused by the rotor model, presumably associated with the stall characteristics of the rotor. That the measured loads in airplane mode ($\alpha_P = 0$) are higher than predicted, might be because of interference with the flow field produced by the wing, an effect that is not included in the analysis and is not present in the wind-tunnel configuration either (fig. 3).

The oscillatory pitch-link loads in flight are always underpredicted (fig. 26), although the trends are predicted well except at the highest speeds for each nacelle angle. Generally this correlation between analysis and measurement is similar to the wind-tunnel results.

AEROELASTIC STABILITY RESULTS

Aeroelastic stability results for the XV-15 rotor on a cantilever wing in the wind tunnel are presented in figures 27 and 28. The modal frequency and damping are shown as a function of speed for the three fundamental wing modes (beam bending, chord bending, and torsion). Good correlation between the theory and measurements is shown, based on the post-test values of the wing frequencies and structural damping. However, there is significant scatter in the wing torsion data; there are little damping data for the wing chord mode; and no data are available in the vicinity of a stability boundary, where larger variations of the damping with speed would allow a more critical test of the theory.

Aeroelastic stability data measured on the XV-15 Tilt Rotor Research Aircraft in flight are presented in figures 29 to 35. Frequency and damping of the three fundamental symmetric wing modes and three fundamental antisymmetric wing modes are shown as a function of speed. Reasonable correlation is obtained using the post-test values of the modal frequencies and structural damping in the analysis. Results are also shown using the pretest values for the frequencies (obtained from the NASTRAN analysis) and structural damping (a uniform level of 1% critical). In the flight test data (fig. 29), even the mean values of the frequencies do not show a smooth variation with speed. There is a trend to lower frequency as speed increases, with which the theory agrees. The flight-test data show a trend of increased damping as speed increases, for all modes (figs. 30 to 35); again, the theory predicts this trend. The measured damping data show a very high level of scatter however, and the operating conditions are far enough from any stability boundary that the damping should not vary greatly with speed.

The flight-test data on aeroelastic stability were obtained from two aircraft; for tip Mach numbers of 0.61 and 0.69; for a standard and a soft pylon downstop; for level flight and descents; and for altitudes of 1,500, 3,000, and 4,500 m. The gross weight was 5,900 kg for all cases. The only observable trends in the data were a lower damping of the symmetric wing-beam bending mode in descent, and a lower damping of the symmetric wing torsion mode at a tip Mach number of 0.69. The data scatter was too high to allow other effects to be seen; moreover, in most cases the data do not allow an extensive examination of the influence of one parameter at a time (for example, the aircraft speed tends to increase as the

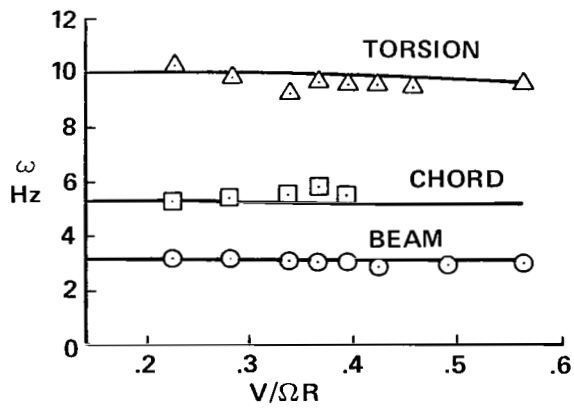

Figure 27.– Cantilever wing mode frequency as a function of speed for $M_{tip} = 0.53$; comparison of wind-tunnel test and calculated results.

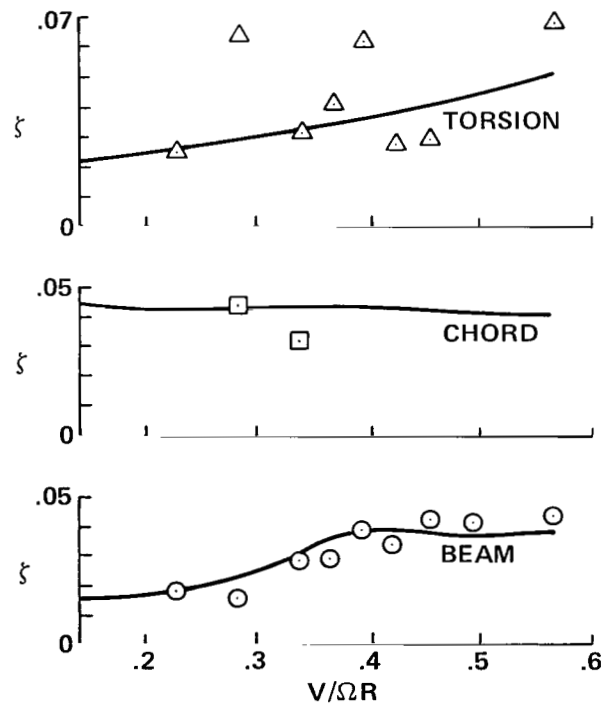

Figure 28.– Cantilever wing mode damping as a function of speed for $M_{tip} = 0.53$; comparison of wind-tunnel test and calculated results.

altitude increases). The mean data shown in figures 29 to 35 are obtained by averaging 1 to 12 points at each speed (excluding only the data for the symmetric beam mode in descent and the symmetric torsion mode at 0.69 tip Mach number). However, averaging frequency and damping measurements cannot be expected to eliminate all errors. The standard deviation of the sample mean is even less meaningful in this case, but it does serve to characterize the scatter of the data. The standard deviation of the mean value is 0.07 to 0.20 Hz for the frequency, and 0.004 to 0.005 for the damping. As for the wind-tunnel measurements, the symmetric wing-bending mode data are of higher quality, with standard

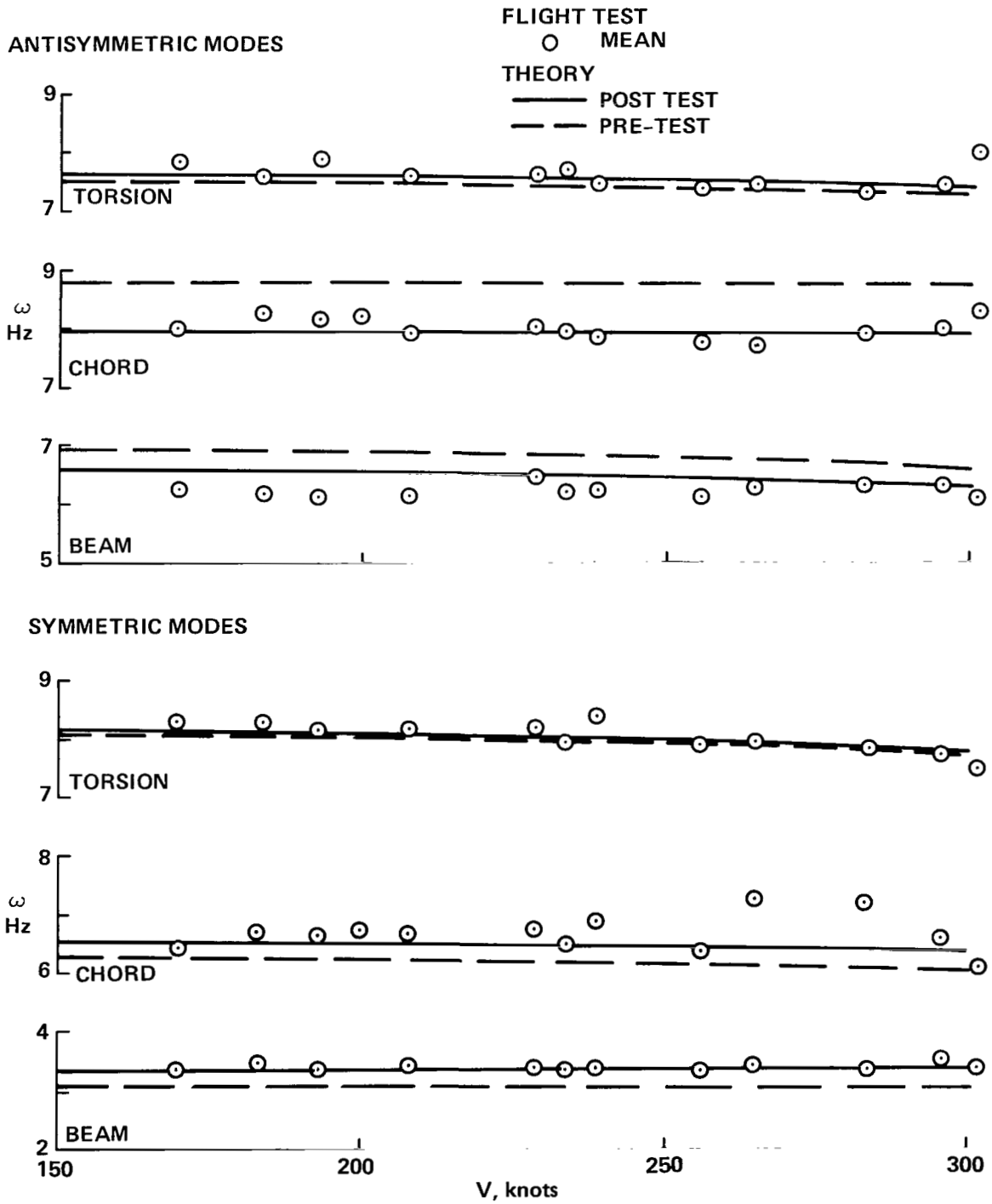

Figure 29.– Airframe mode frequency as a function of speed; comparison of flight test and calculated results.

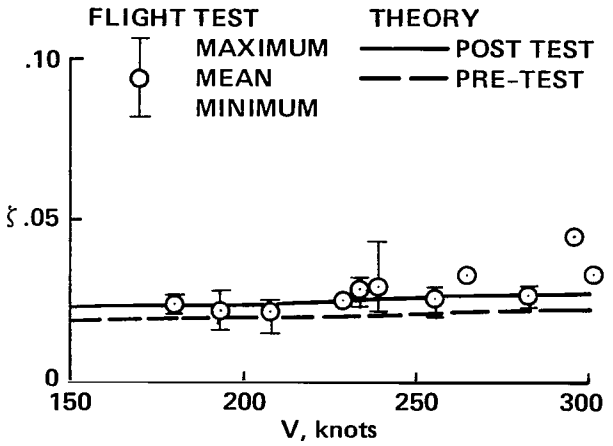

Figure 30.– Airframe symmetric beam mode damping as a function of speed; comparison of flight test and calculated results.

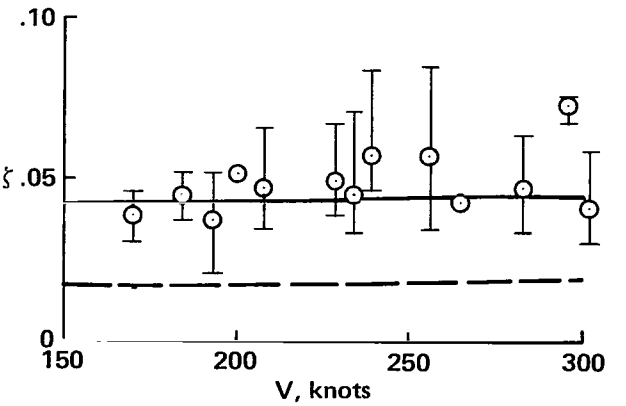

Figure 31.– Airframe symmetric chord mode damping as a function of speed; comparison of flight test and calculated results (see fig. 30 for key).

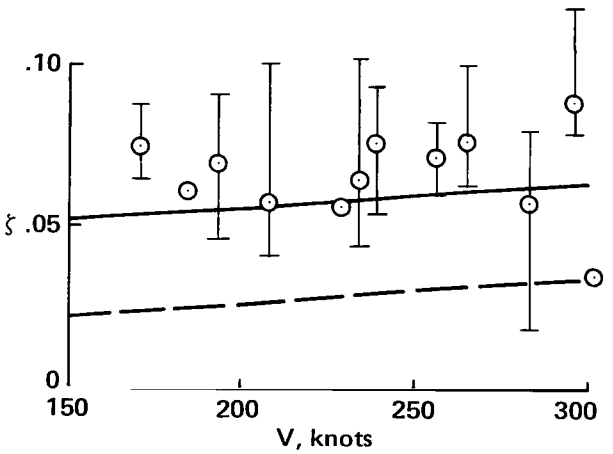

Figure 32.– Airframe symmetric torsion mode damping as a function of speed; comparison of flight test and calculated results (see fig. 30 for key).

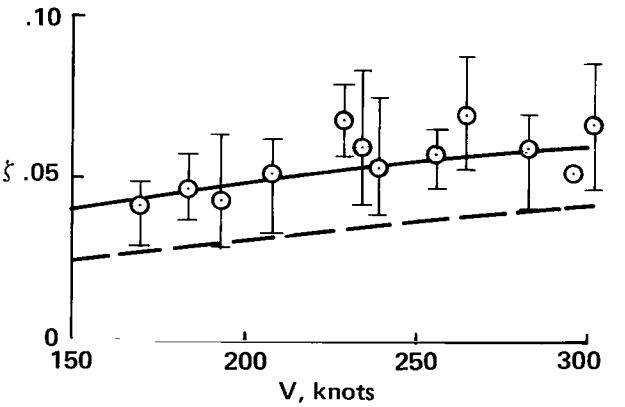

Figure 33.– Airframe antisymmetric beam mode damping as a function of speed; comparison of flight test and calculated results (see fig. 30 for key).

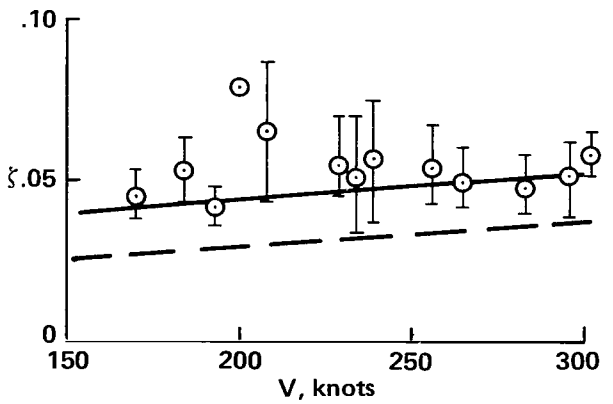

Figure 34.– Airframe antisymmetric chord mode damping as a function of speed; comparison of flight test and calculated results (see fig. 30 for key).

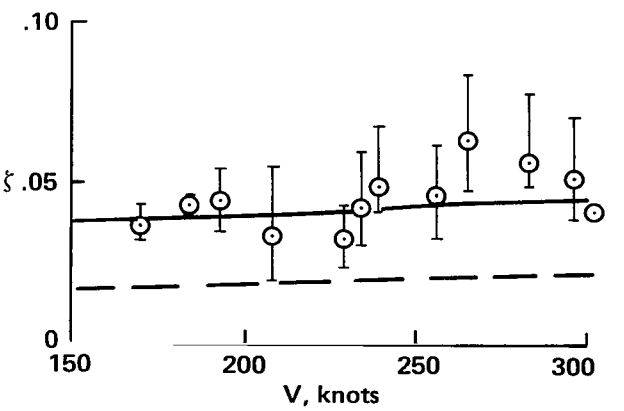

Figure 35.– Airframe antisymmetric torsion mode damping as a function of speed; comparison of flight test and calculated results (see fig. 30 for key).

deviations in frequency and damping approximately one-half the lower values given above.

The calculations presented in figures 29 to 35 were performed for a gross weight of 5,900 kg, a tip Mach number of 0.61, and an altitude of 3,000 m. The theory confirms the small influence of altitude on the damping level for the speeds shown. The damping ratio would be at most 0.002 lower at 4,500 m altitude, and higher by about the same amount at 1,500 m. Such a small effect would be masked by the scatter in the data.

The calculated stability boundaries for the XV-15 in flight are shown as a function of speed and altitude in figure 36. At high altitudes, the stability boundary is at a speed beyond where the analysis predicts the aircraft can achieve a trimmed, equilibrium flight condition. The flight-test data points (all stable) are also plotted. The calculated boundaries are shown for level flight; for a dive at zero power (windmilling rotors); and for a dive at the maximum allowable rotor mast torque of 14,700 N-m (the XV-15 is power-limited only above about 4,750 m altitude). For clarity, only the post-test calculations are shown for the windmilling dive case. In particular, the small differences between the pretest and post-test predictions of the stability boundaries should be noted.

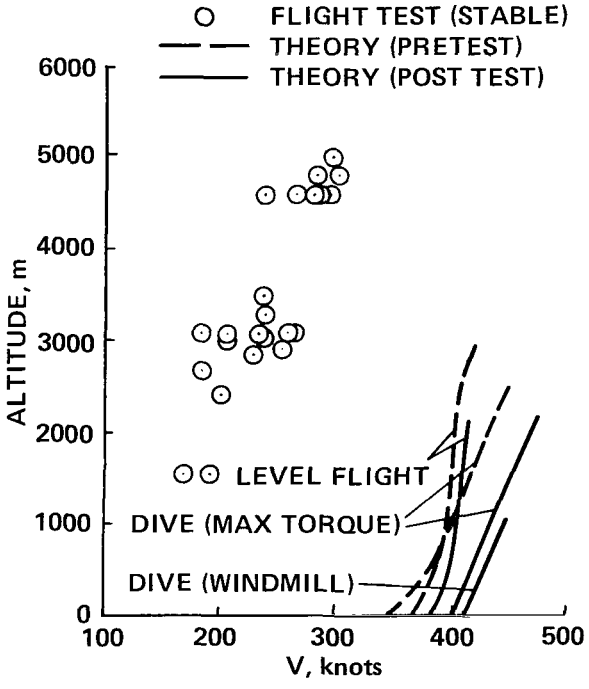

Figure 36.— Aircraft stability boundary as a function of speed and altitude; comparison of flight-test conditions and calculated stability boundaries.

GENERAL ASSESSMENT OF TECHNOLOGY STATUS

The technical problems facing the development of a tilting prop-rotor aircraft are similar to those involved in the development of conventional helicopters. The special characteristics of the tilt rotor configuration do not introduce new subjects, but they can change the emphasis when they are compared to helicopter technology. Moreover, the design parameters of tilt rotors are sufficiently different from conventional helicopter rotors to require test data and analysis development specifically for this concept.

Rotor Performance

The inherent compromise between hover and cruise aerodynamics of the prop-rotor means that the blade loading will not be close to ideal for either. More importantly, it will not be close to the loading typical of either helicopter rotors or airplane propellers. Thus the significant advances in prediction capability for the performance of hovering rotors or propellers that have been made in the last decade are not entirely transferable to tilt rotors. Generally, the level of prediction capability for tilt rotors is somewhat less than it is for helicopter rotors.

Aircraft Performance

The tilt rotor configuration does present some unique airframe aerodynamic problems, such as the design of the nacelles, tail, and wing/fuselage junction. In addition, there is not a long history of successful aerodynamic design solutions for tilt rotors, as there is for airplanes and helicopters.

Vibration

Basically the tilt rotor configuration eliminates most concerns with fuselage vibration. Even in helicopter mode, the wing dynamics provide some vibration absorption. By tilting the rotors, the wake-induced vibration at low speed can be minimized, and the rotor is not intended to fly edgewise at high speeds where the vibration could be high. So while prediction of tilt rotor vibration would be no better than for helicopters, this deficiency is of much less concern.

Rotor Loads

Generally, the prediction capability is at about the same level as for helicopters: a fairly accurate prediction of mean and oscillatory loads is possible. The configuration makes high speed loads of less concern, but rotor loads can define

the upper limit of the conversion corridor. This level of capability is adequate to design a rotorcraft, but still requires considerable wind-tunnel testing to confirm or revise the design loads.

Airframe Loads

Oscillatory loads and vibration in the airframe, particularly the nacelle and wing, can be a problem and are difficult to predict. A structural design that alleviates both the problem and the need for extremely accurate predictions is desirable.

Noise

The high inflow ratio of the tilt rotor eliminates the wake interference and smooths the airload distribution. Also, tilt rotor blades tend to have small cross-sectional area at the tips, minimizing the high-speed noise. Hence, the tilt rotor is basically a quiet rotorcraft configuration, although the high-disk loading tends to increase the noise. The prediction problem is probably easier than for helicopters, but the accuracy of a noise prediction would still not be good.

Rotor Stability

Prediction of the aeroelastic stability of the tilt rotor blades is perhaps more difficult than for helicopter blades, because of such additional considerations as the large collective pitch and rotor speed ranges over which a tilt rotor must operate. Even a gimballed prop-rotor is more accurately compared to a hingeless rotor than to a teetering helicopter rotor when assessing the dynamic characteristics. Hence, as for helicopters, the status of the prediction methodology may be characterized as a lack of confidence that introduces uncertainties in the dynamic behavior of any new rotor configuration. The problems with blade dynamics predictions are more important for tilt rotors since the articulated configuration is not as practical as it is for helicopter rotors.

Whirl Flutter

The coupled rotor/fuselage aeroelastic stability has received a great deal of attention over the last decade. While it remains a critical problem for tilt rotor designs, considerable confidence in the prediction capability has been accumulated. New tilt rotor designs that expand the operational capability of the configuration will, however, introduce new factors that will require further development of the stability analyses. In particular, significantly increasing the speed capability of tilt rotors will require better treatment of high speed aerodynamic effects on the rotors.

Aerodynamic Interference

The interactional aerodynamics problems may be somewhat simpler than for helicopters, but there has also been less work on these problems for tilt rotors. In any case, adequate analytical techniques for the aerodynamic interference between the rotor and airframe have not yet been developed.

Gust Alleviation

The gust response of the tilt rotor configuration is different qualitatively, but not quantitatively, from helicopters. The capability to predict the gust response is reasonably good, because of the simpler aerodynamics of the rotors in cruise flight. A number of gust alleviation controllers have been designed and tested, some successfully, but none has been tested in flight.

Flutter Control

Very little work on design or testing of automatic control systems for flutter control of tilt rotor aircraft has been done. A simple design has been tested full scale in the wind tunnel, and many gust alleviation systems also increase the whirl flutter stability of the aircraft. The analytical design tools are available for this problem, but application to a tilt rotor is not a trivial step, when the critical nature of a flutter control system is considered.

Data Base

Most of the testing of tilt rotor models and aircraft over the last fifteen years has been for the XV-15 aircraft development program. Hence, in spite of the large number of tests there is not that much data available that has the high quality and detailed documentation required for development of analyses, verification of analyses, or examination of parameter variations.

CONCLUSIONS

Calculated performance, loads, and stability of the XV-15 Tilt Rotor Research Aircraft have been compared with wind-tunnel and flight measurements. The performance data included power and efficiency, in both hover and cruise. The rotor loads data consisted of the oscillatory beam and chord bending moments, and the oscillatory pitch link loads. The aeroelastic stability data included the frequency and damping of the fundamental wing modes.

The correlation between the measured and predicted results can be summarized as follows. For performance, there was a moderate level of scatter in the data, which consisted only of rotor thrust and power information. Good correlation was achieved, based on proper choice of the empirical induced-velocity factor for the hovering rotor, the airframe download in hover, and the airframe drag in cruise. For loads, there was a moderate level of scatter in the data, which consisted only of one-half peak-to-peak information. Fair to good correlation was obtained, using an empirical factor for the induced velocity in helicopter forward flight, and static stall for the blade airfoil characteristics. The oscillatory beam bending moments were predicted well; the oscillatory chord bending moments were sometimes predicted well and sometimes underpredicted; the oscillatory pitch-link loads were always underpredicted. Some anomalous results were seen (such as the not insignificant oscillatory loads at zero nacelle angle), and there was a general tendency for the predicted loads to increase less than the measurements at high speeds (presumably because of the stall model). For stability, there was a very high level of scatter in the data, which consisted of only frequency and damping information at speeds well below any stability boundary. Good correlation was achieved, using the post-test values of the frequencies and structural damping. The pretest values produced a reasonable prediction of the stability boundaries. Based on this correlation, the analysis may be assessed overall as adequate for reliable use in the design, evaluation, and testing of tilting prop-rotor aircraft.

Regarding future methodology development, there are clear opportunities for improvements in certain areas. For performance, a hover analysis using nonuniform inflow is needed. The low aspect ratios of future tilt rotor designs may make lifting surface techniques desirable as well. A method for calculation of the airframe download in hover is required, in addition to current efforts to develop wing configurations with low download. For loads, it may be expected that good nonuniform inflow and dynamic stall models would improve the predictions. The current inflow and stall models are all empirical to some extent; thus, these models have not been developed for the aerodynamic environment that characterizes tilting prop-rotors, so some development specifically for tilt rotors is needed. For stability, reliable pretest predictions of the structural dynamics of the airframe are needed, particularly frequencies and mode shapes. An improved capability to handle new rotor configurations, such as bearingless rotors, is desired as well.

Better experimental data are needed to support the development and verification of tilting prop-rotor prediction capability. More accurate and detailed data are needed. The data currently available for the XV-15 shows significant scatter in most cases, and often were not acquired at consistent operating conditions. For performance, direct measurements of the airframe hover download and cruise drag are required, as well as rotor blade airload measurements. For loads, time-history data and rotor blade airload measurements are needed. For stability, measurements of the flutter mode shapes and measurements closer to stability boundaries are required.

Ames Research Center
National Aeronautics and Space Administration
Moffett Field, California, 94035, June 15, 1983

REFERENCES

1. Johnson, W.: Development of a Comprehensive Analysis for Rotorcraft. Vertica, vol. 5, nos. 2 and 3, 1981.
2. Johnson, W.: A Comprehensive Analytical Model of Rotorcraft Aerodynamics and Dynamics. NASA TM-81182, June 1980.
3. Bell Helicopter Company: Advancement of Proprotor Technology – Design Study Summary. NASA CR-114682, Sept. 1969.
4. Johnson, W.: Analytical Modeling Requirements for Tilting Proprotor Aircraft Dynamics. NASA TN D-8013, July 1975.
5. Harendra, P. B.; Joglekar, M. J.; Gaffey, T. M.; and Marr, R. L.: V/STOL Tilt Rotor Study – A Mathematical Model for Real Time Flight Simulation of the Bell Model 301 Tilt Rotor Research Aircraft. NASA CR-114614, April 1973.
6. Maisel, M. D.: Tilt Rotor Research Aircraft Familiarization Document. NASA TM X-62407, Jan. 1975.
7. Bell Helicopter Company: Advancement of Proprotor Technology – Wind Tunnel Test Results. NASA CR-114363, Sept. 1971.

1. Report No.	2. Government Accession No.	3. Recipient's Catalog No.
NASA TP -2291		

4. Title and Subtitle	5. Report Date
AN ASSESSMENT OF THE CAPABILITY TO CALCULATE TILTING PROP-ROTOR AIRCRAFT PERFORMANCE, LOADS, AND STABILITY	March 1984
	6. Performing Organization Code
7. Author(s)	8. Performing Organization Report No.
Wayne Johnson	A-9411
	10. Work Unit No.
9. Performing Organization Name and Address	T-5061YA
NASA Ames Research Center Moffett Field, Calif. 94035	11. Contract or Grant No.
	13. Type of Report and Period Covered
12. Sponsoring Agency Name and Address	Technical Paper
National Aeronautics and Space Administration Washington, D.C. 20546	14. Sponsoring Agency Code 505-42-11

15 Supplementary Notes

Point of Contact: Wayne Johnson, Ames Research Center, M/S 247-1, Moffett Field, Calif. 94035
(415) 965-5043 or FTS 448-5043

16. Abstract

Calculated performance, loads, and stability of the XV-15 Tilt Rotor Research Aircraft are compared with wind-tunnel and flight measurements, to define the level of the current analytical capability for tilting prop-rotor aircraft, and to define the requirements for additional experimental data and further analysis development. The correlation between calculated and measured behavior is generally good, although there are some significant discrepancies. Based on this correlation, the analysis used is assessed overall as being adequate for the design, evaluation, and testing of tilting prop-rotor aircraft. A general assessment of the state of the art of tilt rotor predictive capability is given. Specific areas are identified where improvements in the capability to calculate performance, loads, and stability are desirable. Requirements for more accurate and detailed data which support the development of improved analytical models are identified as well.

17. Key Words (Suggested by Author(s))	18. Distribution Statement
Tilting prop-rotor XV-15 aircraft Rotorcraft analysis	Unclassified - Unlimited Subject Category – 05

19. Security Classif. (of this report)	20. Security Classif. (of this page)	21. No. of Pages	22. Price*
Unclassified	Unclassified	21	A02

*For sale by the National Technical Information Service, Springfield, Virginia 22161

NASA-Langley, 1984

2 1 1J,A, 840222 S00903DS
DEPT OF THE AIR FORCE
AF WEAPONS LABORATORY
ATTN: TECHNICAL LIBRARY (SUL)
KIRTLAND AFB NM 87117